Journal Pre-proof

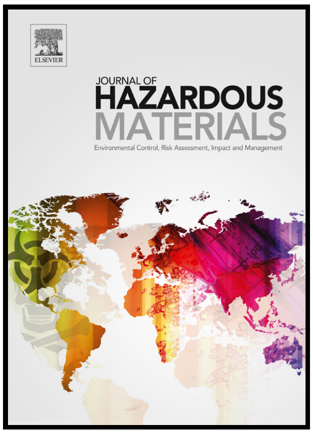

Two sides of the same coin: weathering differences of plastic fragments in coastal environments around the globe

Bo Hu, Mui-Choo Jong, João Frias, Irina Chubarenko, Gabriel Enrique De-la-Torre, Prabhu Kolandhasamy, Md. Jaker Hossain, Elena Esiukova, Lei Su, Hua Deng, Wenjun Zhao, Yifan Zheng, Huahong Shi

PII: S0304-3894(24)03538-6

DOI: https://doi.org/10.1016/j.jhazmat.2024.136957

Reference: HAZMAT136957

To appear in: *Journal of Hazardous Materials*

Received date: 30 September 2024
Revised date: 8 December 2024
Accepted date: 19 December 2024

Please cite this article as: Bo Hu, Mui-Choo Jong, João Frias, Irina Chubarenko, Gabriel Enrique De-la-Torre, Prabhu Kolandhasamy, Md. Jaker Hossain, Elena Esiukova, Lei Su, Hua Deng, Wenjun Zhao, Yifan Zheng and Huahong Shi, Two sides of the same coin: weathering differences of plastic fragments in coastal environments around the globe, *Journal of Hazardous Materials,* (2024) doi:https://doi.org/10.1016/j.jhazmat.2024.136957

Two sides of the same coin: weathering differences of plastic fragments in coastal environments around the globe

Bo Hu [a], Mui-Choo Jong [b], João Frias [c], Irina Chubarenko [d], Gabriel Enrique De-la-Torre [e], Prabhu Kolandhasamy [f], Md. Jaker Hossain [a, g], Elena Esiukova [d], Lei Su [a, h], Hua Deng [a, i], Wenjun Zhao [a], Yifan Zheng [a, j], Huahong Shi [a,*]

[a] State Key Laboratory of Estuarine and Coastal Research, East China Normal University, Shanghai 200241, China

[b] Institute of Environment and Ecology, Tsinghua Shenzhen International Graduate School, Tsinghua University, Shenzhen 518055, China

[c] Marine and Freshwater Research Centre (MFRC), Atlantic Technological University (ATU), Galway Campus, Dublin Road, Galway H91 T8NW, Ireland

[d] Shirshov Institute of Oceanology, Russian Academy of Sciences, 36, Nakhimovsky Prosp., Moscow 117997, Russia

[e] Grupo de Investigación de Biodiversidad, Medio Ambiente y Sociedad, Universidad San Ignacio de Loyola, Lima, Peru

[f] Department of Marine Science, School of Marine Sciences, Bharathidasan University, Tiruchirappalli, Tamil Nadu 620024, India

[g] Institute of Marine Sciences, University of Chittagong, Chittagong-4331, Bangladesh

[h] College of Oceanography and Ecological Science, Shanghai Ocean University, Shanghai 201306, China

[I] Key Laboratory of Marine Mineral Resources, Ministry of Natural Resources, Guangzhou Marine Geological Survey, China Geological Survey, Guangzhou, 511458, China

[j] Chinese Research Academy of Environmental Sciences Tianjin Branch, Research Institute for Environmental Innovation (Tianjin Binhai), Tianjin 300450, China

Address all correspondence to: State Key Laboratory of Estuarine and Coastal Research, East China Normal University, Shanghai 200241, China;

hhshi@des.ecnu.edu.cn

Abstract

Plastic debris in coastal environments usually undergoes weathering due to various environmental conditions. However, the weathering effects on exposed and shaded sides of the same plastics are underexplored. In this study, 1573 plastic fragments were collected from 15 coastal sites worldwide between December 2021 and December 2022, and weathering experiments were conducted outdoors. The field investigation showed significant two-sided weathering differences of plastic fragments. The weathering morphology included biota, cracks, delamination, discoloration, etc. The weathering degree was assessed with three metrics, i.e., line density (0 to 58 mm/mm^2), surface loss (0 to 92%), and texture index (0 to 2). The 3D magnitudes of these three metrics revealed the two-sided weathering differences of plastic fragments. Specifically, 43% of the samples had magnitudes > 5, indicating significant differences. Outdoor simulations suggested that sun-exposed sides developed more cracks, pores, and bubbles, while shaded sides remained smoother. After 12 months, the line density increased from 2.85 to 9.23 mm/mm^2 for polyethylene (PE) and 4.16 to 8.47 mm/mm^2 for polypropylene (PP) ($p < 0.05$). The carbonyl index increased from 0.50 to 1.70 (PE), from 0.18 to 1.10 (PP), and from 0.45 to 1.57 (polyvinyl chloride). This increase indicated oxidative degradation on sun-exposed sides. Our results highlighted the uneven degree of weathering on both sides of the same plastic fragment due to different environmental factors. The study provided critical insights for creating more accurate models to predict plastic degradation, which will help inform global strategies to reduce plastic pollution.

Keywords: Plastic fragments, coastal environment, surface aging features, weathering differences

1. Introduction

Plastic pollution has become a critical environmental issue due to the prolonged rise in global plastic production and consumption. Approximately 8-12 million metric tons of plastic enter the oceans annually, contributing significantly to marine debris [1]. When mismanaged and discarded plastic debris accumulates in the environment, it usually undergoes weathering and breaks into smaller fragments due to environmental stress [2,3]. Moreover, these plastic products typically break into small pieces of 5 mm to 25 cm [4]. The widespread distribution of plastic debris on beaches causes damage to marine ecosystems and poses potential risks to human health [5,6]. Plastic fragments serve as transitional forms between larger plastic debris and micro/nanoplastics (MNPs) to understand the release of smaller particles into the environment [4,7]. Therefore, it is crucial to study the weathering and fragmentation of plastic fragments to assess their broader environmental impact.

The weathering process of plastic fragments in beach environments is primarily driven by ultraviolet (UV) radiation, mechanical abrasion, and biodegradation [8,9]. When plastic fragments undergo natural aging, their surface weathering features become increasingly complex [10]. Generally, plastics develop cracks, pits, holes, and other surface aging morphology [11]. Previous studies revealed a strong correlation between UV exposure and surface morphology in plastics. For example, polystyrene fragments exhibit surface cracks after 8 weeks of weathering, but UV exposure causes comparable damage to polyethylene terephthalate and polyvinyl chloride (PVC) in just 7 days [12,13]. In our previous works, crack line density has been proven to be a valuable metric for assessing the weathering of plastic fragments [14]. Furthermore, the structure of plastic changes under various environmental conditions, which may result in distinct morphological and chemical alterations, such as a reduction in crystallinity [15,16]. For instance, foam floating on the sea surface is often in a state that one side exposed to the irradiation of the sun and the other is immersed in seawater. This state is likely to lead to significant differences of the changes between the sides of the foam foams [17].

So far, it is still unclear if there is a surface difference in the weathering degree of the same sample of the hard plastic fragments. More research focuses solely on the surface changes of one side of plastic fragments and overlooks the other side. This one-sided approach restricts the understanding of plastic aging and degradation processes. It largely neglects the influence of different environmental conditions (e.g., the periodic variation of waves) on the opposite surfaces of the fragments. A comprehensive study of the differences between both sides of plastic fragments is crucial for uncovering the natural mechanisms of aging and fragmentation.

In this study, we conducted a large investigation on the weathering features of plastic fragments worldwide and outdoor weathering experiments. We aimed to determine whether weathering differences existed between the two sides of plastic fragments and to explore the underlying reasons for these differences. The results will improve our understanding of plastic fragment aging and fragmentation mechanisms. It also provided valuable insights for mitigating plastic pollution by presenting a more accurate pattern of plastic degradation in the environment.

2 Methods and materials

2.1 Sampling areas and sample collection

Between December 2021 and December 2022, massive visually identifiable plastic fragments were collected from 15 coastal sites (**Fig. 1**). These fragments typically have a width-to-height ratio >10 and uniform thickness with no curling. Based on OSPAR [18], we did the sampling work following the actual situation. Specifically, a 100-meter section of the coastline was randomly selected at each site, and all visible plastic fragments within this area were collected. This involved visually scanning the beach surface and carefully retrieving fragments directly from the uppermost layer of sediment. In addition, fragments were sorted in aluminum foil bags and labeled with the sample site information for later analysis. Several quality control measures were employed to maintain sample integrity and prevent cross-contamination. Each fragment was handled with clean stainless-steel forceps to avoid contamination between samples.

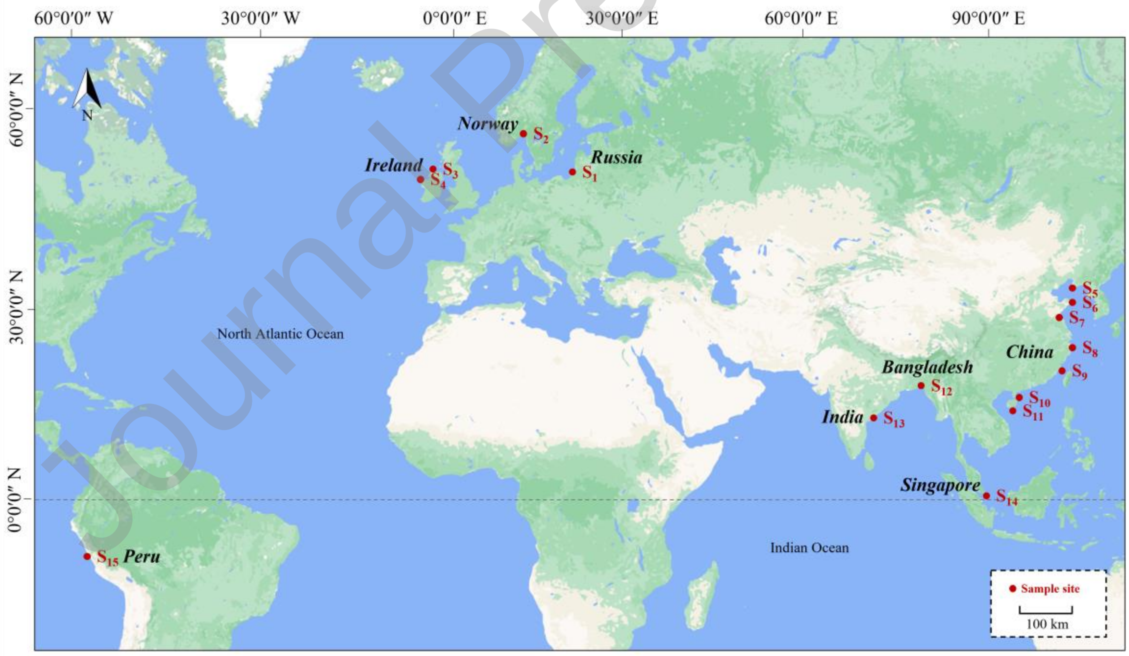

Fig. 1. Map of sampling locations.

2.2 Preprocessing and image acquisition of plastic fragments samples

The plastic samples were categorized according to the presence or absence of visible biological or unidentified material attachments. Plastic fragments with visible attachments were stored separately in labeled zip-lock bags. The remainder of the samples were thoroughly cleaned with anhydrous ethanol and 30% hydrogen peroxide before storage. Both sides of each plastic fragment were photographed for overall appearance and microscopic images. For overall appearance images, macro photography was taken using an 8.5-megapixel digital camera (Sony FDR-AX60) to capture high-resolution images. According to these images, the dimensional characteristics (i.e., thickness, Feret diameter, and color) of each plastic fragment were measured and recorded. Thickness (mm) was measured using a vernier caliper, while the Feret. diameter (Feret., mm^2) was determined using ImageJ software (version 3.2.34). Microscopic images were photographed using a Zeiss Discovery V8 microscope (Carl Zeiss Micro Imaging GmbH, Göttingen, Germany) with CapStudio software with 5x magnification. Each fragment was photographed on both sides, and the number of images per sample varied depending on the size of the plastic fragment. These microscopic images facilitated the identification of weathering features such as cracks, delamination, bio-adhesion, and discoloration on both sides of the fragments.

2.3 Identification of polymer types in beach plastic fragments

A Fourier Transform Infrared Spectrometer (FTIR; Thermo Fisher Scientific, Nicolet iN10, USA) and a micro-Fourier Transform Infrared Spectrometer (μ-FTIR; Thermo Fisher Scientific, Nicolet iN10, USA) were employed to determine the polymer composition of all plastic fragment samples. Most samples were analyzed using the FTIR in Attenuated Total Reflectance (ATR) mode, with an 8-second scanning time. ATR mode was selected for its ability to mitigate issues with the carbonyl peak's high extinction coefficient to ensure more precise polymer identification

[19]. Those samples smaller than 2.5 mm were analyzed using μ-FTIR. This method allowed for a scanning time of 16 seconds at a resolution of 4 cm^{-1}. Each sample was scanned at least three times. All spectra was matched against Thermo Fisher's commercial spectral library, and a match of 70% or higher was deemed sufficient for reliable polymer identification [20,21].

2.4 Outdoor weathering experiment for plastic fragments

For the outdoor weathering experiment, we selected three common blue plastic materials frequently found in plastic debris, i.e. polyethylene (PE), polypropylene (PP), and PVC. All materials were sourced from *Pepe Plastic Material Company* (China) to ensure consistency in quality and shade across the samples. Each material was cut into sheets measuring 12 cm by 4 cm and 1 mm thick. Three replicates were set up for each plastic type, and the materials were mounted on stainless steel frames by clips (**Fig. S1**). The setup positioned one side of each plastic piece toward the sun while the other faced the shade. It simulated the uneven solar intensity experienced on both sides in a natural environment. The mean annual solar radiation intensity was 4.47 ± 1.04 kWh in the experimental area. This value closely matched the solar intensities at field sample sites S8 and S9, where the intensities were 4.55 kWh and 4.94 kWh, respectively (**Table S1**). Samples were collected for imaging analysis at 8 and 10 months. In addition, we examined the infrared spectra using FTIR and calculated the carbonyl index (CI) using SpectraGryph 1.2 software. Data extraction and calculation methods for weathering experiments were performed similarly in plastic fragments from beach environments.

2.5 Quantitative metrics for texture characteristics of plastic fragments

Three key metrics were employed to quantify the surface weathering features of plastic fragments. (1) Crack line density (mm/mm^2) referred to the total crack length within a specified area. Original color images were converted into 8-bit grayscale and then binarized using an appropriate threshold to distinguish cracks from intact areas. (2) Surface loss (%) referred to the proportion of the damaged or lost area of the plastic fragments relative to the total sample area. (3) The texture index quantifies irregular surface variations that extended beyond visible morphological features such as cracks, delaminations, and pits. It was difficult to capture these subtle variations with standard segmentation methods, so they were analyzed using the gray-level co-occurrence matrix (GLCM) in MATLAB. First, the images were imported and converted to an 8-bit format. Then, the "graycomatrix" and "graycoprops" functions were used to generate the matrix and extract feature vectors. While GLCM was used to calculate multiple texture parameters, the focus was on “entropy” and “contrast”, which best capture surface irregularities. The GLCM method is robust across different images, and the algorithm was simple and easy to implement. Therefore, the texture index was calculated by multiplying “entropy” and “contrast”. Compared to traditional methods, this metric precisely measured complex surface features. Using the image textures of plastic fragments to quantify the physical degradation characteristics of different polymers offered a comprehensive perspective on natural aging properties. We could compare weathering characteristics across scales and establish a meaningful connection between morphological and chemical change (**Text S1**).

It is important to note that not all plastic fragments in the sample exhibited cracks or surface loss. It meant that the sole index could not be enough to represent all surface morphologies. To solve this problem, this study conducted a comprehensive 3D analysis, with line density, surface loss, and texture index assigned to the x, y, and z axes, respectively. The overall surface complexity of the plastic fragments was quantified by calculating the "Magnitude", and the distance from each (x, y, z) coordinate to the origin (0, 0, 0). The equation is as follows (1):

$$\text{Magnitude} = \sqrt{Line\ density^2 + Surface\ loss^2 + Texture\ index^2} \qquad (1)$$

Equation (1) consolidates the three metrics into a single value, providing an overall measure of surface texture complexity. This study presented these metrics in a multidimensional space, a common approach to better capture the intricacies of surface features [22,23].

2.6 Data analysis

Statistical analyses and graph generation were performed using SPSS Statistics 20 (IBM Corp., Armonk, NY, USA), MATLAB R2020b, and Origin2024 (OriginLab, Massachusetts, USA). The normality of the metric data for crack line density, surface loss, and texture index was assessed using the Shapiro–Wilk test. The Kruskal–Wallis non-parametric test was applied to examine for non-normally distributed data.

3 Results and discussion

3.1 Divergent weathering changes on two sides of plastic fragments

In the current study, the plastic fragments were predominantly composed of PE (46%) and PP (48%) (**Fig. S2 A**). Over half (52.4%) of samples had a thickness of 0.5–1.5 mm and nearly half (47.8%) measured 10–20 mm in size (**Fig. S2 B, C**). Blue and white fragments were the most common (**Fig. S2 D**). The surface of these plastic fragments exhibited various morphological features such as cracks, delamination, chalking, and wrinkles (**Fig. S3**). These weathering features exhibited significant differences on both sides of the plastic fragments. Three typical types of two-sided differences were observed, i.e., presence or absence of bio-adhesion (**Fig. 2 A**, **B**), distribution of weathering features such as cracks and delamination (**Fig. 2 C-F**), and color changes with one side showing noticeable discoloration (**Fig. 2 G, H**).

The uneven environmental stress contributed significantly to differences observed between the two sides of plastic fragments. Typically, drifting and flipping caused by wind, water currents, and biological attachment result in different levels of exposure on each side [24,25]. For instance, wave action exerted mechanical and chemical erosion on the surface of plastic fragments, making the surface rougher and gradual decomposition [26]. Moreover, nutrients, moisture, and oxygen support the biofilms on plastic surfaces in marine environments [27,28]. The bacteria and fungi enhance the growth of biofilms, especially in warm, humid conditions and appropriate temperatures [29,30]. Prolonged exposure to UV radiation on plastic fragments made the polymer chains broken on the exposed side and the surface rougher over time [31]. Salts and chemicals in seawater reacted with the plastic and create a rougher texture on one side, while the other remains smoother [32,33]. High salinity in marine environments led to salt crystallization, accelerate aging and mechanical wear from waves [34,35]. Additionally, photo-oxidation and material stress responses cause color changes on the plastic fragment surfaces and affect properties such as tensile strength and fracture strain [36].

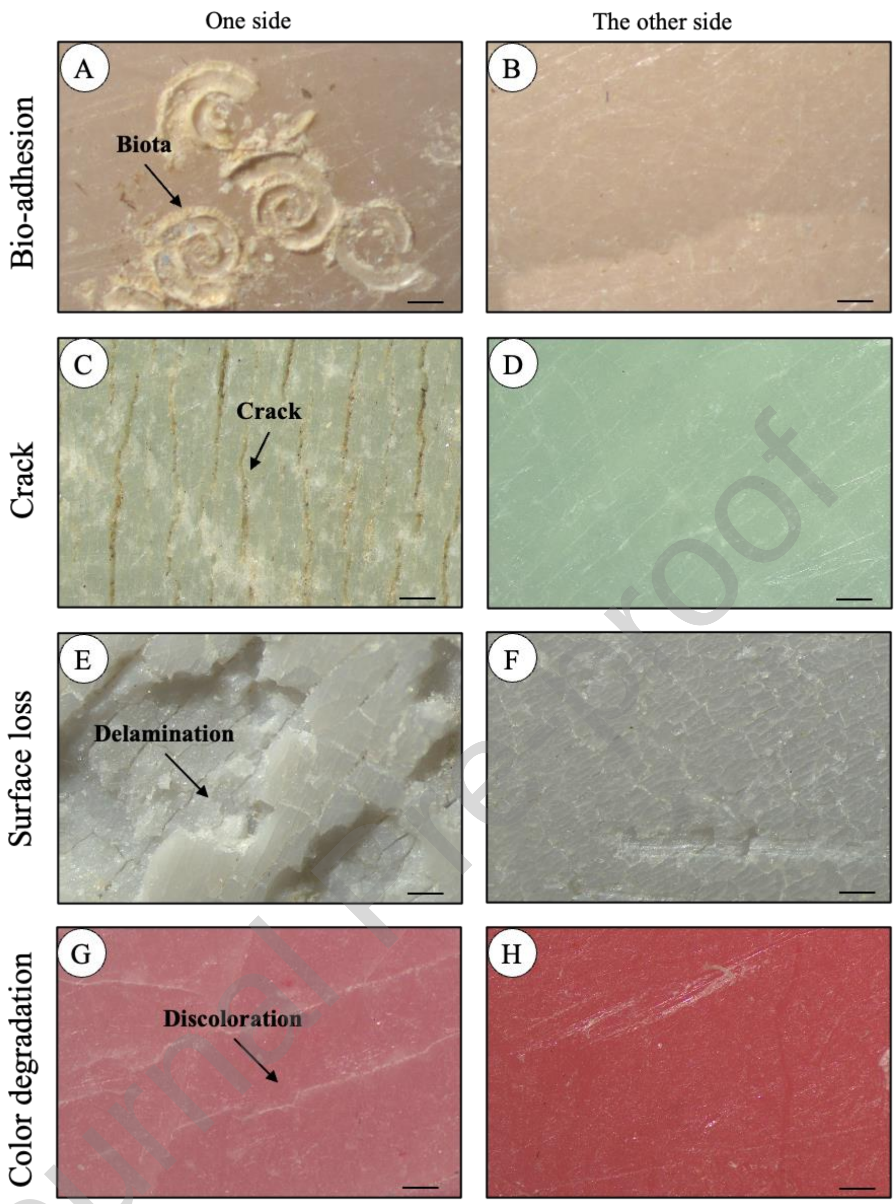

Fig. 2. Typical two-sided difference type of coastal plastic fragments. Biota samples (A, B), visible cracks samples (C, D), delamination (E, F), degradation and discoloration (G, H). Scale bar = 0.5 mm.

3.2 Quantification of weathering differences between two sides of plastic fragments

We used three key metrics to quantify the weathering features of plastic fragments. They were line density, surface loss, and texture index, with values ranging from 0.00 to 58.00 mm/mm², 0.00 to 92.12%, and 0.00 to 1.51, respectively (**Fig. 3**). After the data for each metric was sorted in ascending order, most samples fell within the lower range. Specifically, 69.36% of the samples had a line density between 0–5 mm/mm² (**Fig. 3A**); 65.35% showed surface loss between 0–5% (**Fig. 3B**); and 46.76% exhibited a texture index between 0–0.1 (**Fig. 3C**). The results showed that most fragments had undergone very short environmental expose. This led to limited physical, chemical, or biological degradation, and stable surface characteristics [37]. However, few samples might have undergone prolonged environmental exposure and showed significant altering their surface weathering features [38,39]. Under natural conditions, increased cracking and surface loss caused the surfaces of plastic fragments to become more brittle [40]. This process generated smaller microplastics and increased the risk of toxic substance release in marine life and coastal ecosystems [41]. This observation contrasts with most laboratory studies, which predominantly emphasize parameters such as contact angle, carbonyl index, and crystallinity. Historically, methods for inspecting plastic surfaces have varied significantly, with differences in magnification and examined area, making it challenging to achieve consistent, quantitative assessments. We compared this study with other relevant research in quantitative descriptions of polymer weathering (**Table S2**).

In addition, we analyzed the differences in value in each metric between the two sides to examine the two-side difference. The results showed that about 50% of the plastic fragments had a large two-sided difference (**Fig. 3D-F**). The main cause of this difference was inconsistency in environmental exposure, such as biological oxidation, soil adhesion, and seawater erosion [42-44]. Some samples, however, were supposed to be exposed in different orientations or positions for extended periods, which resulted in one side undergoing more severe external erosion [37].

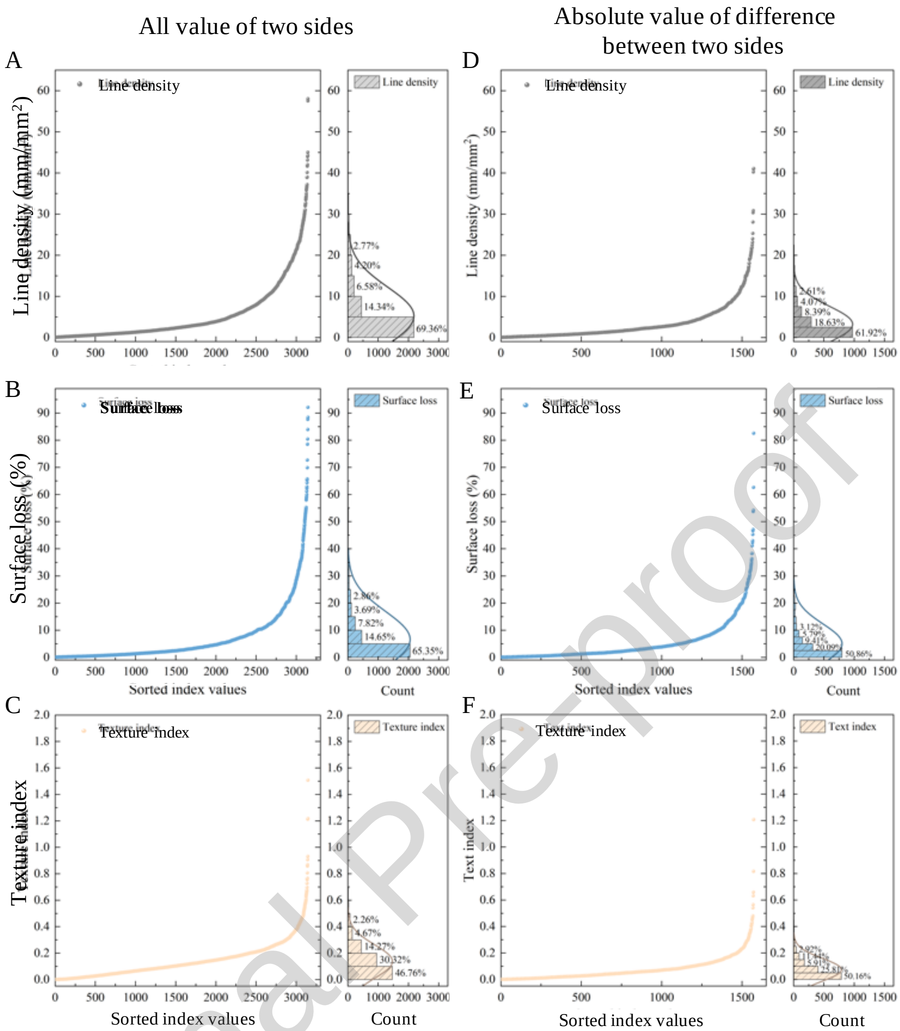

Fig. 3. Distribution of line density, surface loss, and texture index of both surfaces of plastic fragments from coastal environment. Left-hand plots show the sorted distribution of line density (A), surface loss (B), and texture index (C) for both fragment surfaces. Right-hand plots present the sorted absolute differences for the same metrics (D-F). "The sorted index values" refers to the sample numbers organized in ascending order based on the data values.

The three-dimensional comprehensive assessment system was used to quantify the surface texture degree of plastic fragments across three metrics. Results showed that 46.73% of samples had magnitudes between 0 and 5, with the remaining samples having a magnitude above (**Fig. 4 A, B**). The quantification of surface texture in plastic fragments directly reflected their aging degree, i.e., the more complex the texture, the higher the degree of weathering [45]. Furthermore, according to the analysis of two-sided differences, 43.04% of samples had weathering differences >5 (**Fig. 4 C, D**). It was likely due to environmental or physical disturbances. The prevalence of these differences further demonstrated the uneven aging of the two sides of plastic fragments [45]. Multidimensional analysis has been widely applied in neuroscience and big data analytics to manage high-dimensional data efficiently and make intricate patterns more comprehensible [46].

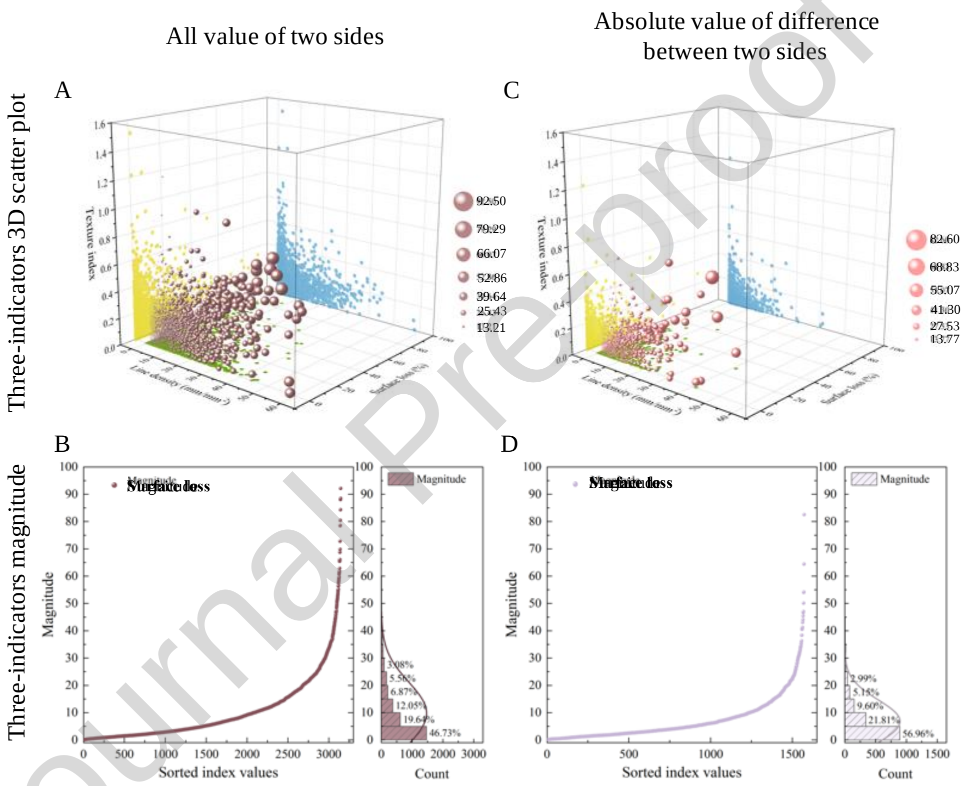

Fig. 4. Three indicator 3D distributions of the quantified surface morphology of beach plastic fragments. (A, B) Value of all indicators; (C, D) Absolute value of difference between two sides. The x, y, and z axes represent line density, surface loss, and texture index, respectively, while the size of the spheres represents a specific quantitative variable, indicating its magnitude in the dataset.

3.3 Outdoor simulation of the difference between two sides of plastic fragments

In outdoor simulation experiments, blue plastic sheets made of PE, PP, and PVC showed distinct differences between the sun and shade sides after outdoor aging (**Fig. 5**). The surfaces of PE and PP showed cracks and craze (**Fig. 5C, I**), and PVC showed bubble-like textures (**Fig. 5O**).

In contrast, the shaded side surfaces displayed only slight discoloration and retained smoother textures (**Fig. 5F, L, R**). Both sides of these materials' initial state were soft and flat with little noticeable differences (**Fig. S4**). Our simulation experiments demonstrated that UV radiation accelerated plastic weathering through photochemical reactions, leading to polymer degradation and oxidation. These effects were especially evident in the color changes, with blue plastics showing the most severe degradation [47]. Sun-exposed surfaces of plastic pieces were more oxidized than shaded surfaces. Specifically, UV-exposed PP syringes became opaque and lost tensile strength after prolonged exposure [48]. The minimal changes on shaded plastic pieces confirm that UV radiation is the primary driver of degradation. UV exposure and high temperatures led to surface cracking through polymer scission, cross-linking, and embrittlement [14,49].

Different plastics showed distinct weathering patterns under sunlight. PE and PP are polyolefins with long hydrocarbon chains and are susceptible to photochemical oxidation and cracking under UV exposure. As observed in previous studies, the exposure leads to molecular chain breakage and the formation of surface cracks and fissures [50]. As for PP, photooxidation of hydrocarbon bonds generates oxidized products such as ketones and aldehydes that accelerate aging [51]. On the contrary, chlorine atoms in the main chain of PVC are somewhat UV-stable. However, they also initiate dehydrochlorination reactions, releasing hydrochloric acid and a bubble-like texture [52]. This can further degrade the surface. Under the combined effects of UV radiation and temperature fluctuations, PE and PP became brittle and developed cracks. Meanwhile, PVC formed a typical bubble-like aging characteristic under similar conditions

[53,54]. Based on our simulation experiments, it can be inferred that the side of the field plastic fragments with cracks, bubbles, or discoloration are more likely to be sun-exposed.

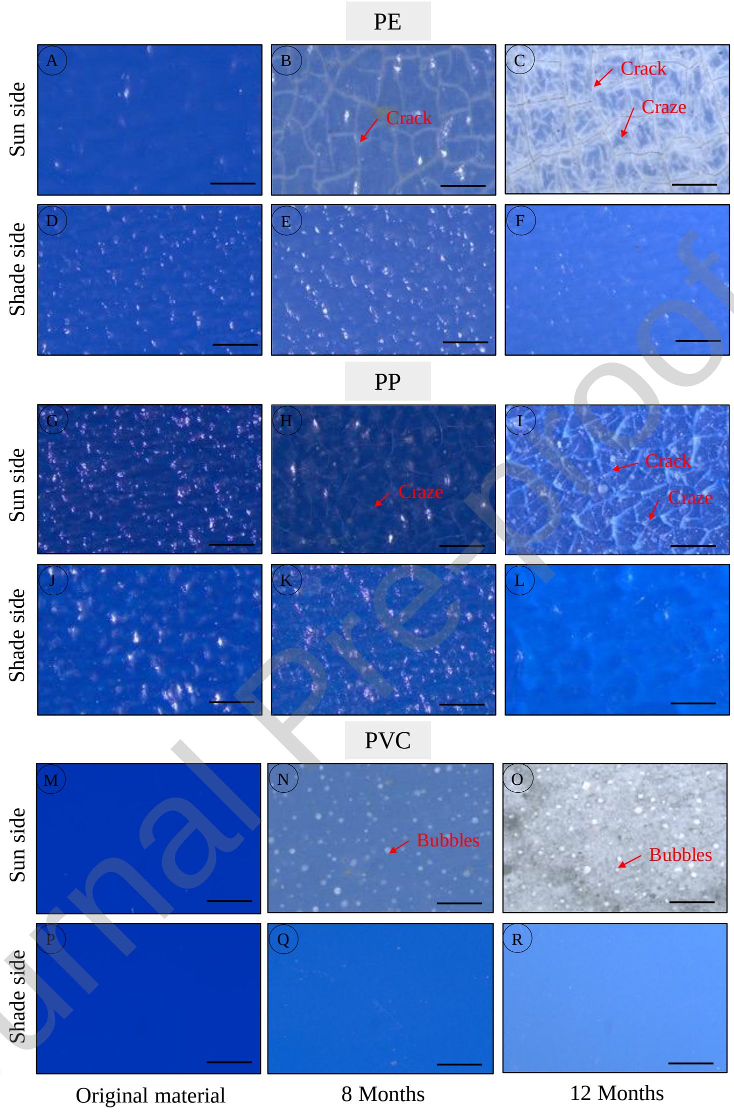

Fig. 5. Surface texture changes of polyethylene (PE), polypropylene (PP), and polyvinyl chloride (PVC) sheets after outdoor aging. The scale bar = 0.5 mm. Craze refers to early microcracks on the surface of materials like plastics.

The main weathering indices of PE, PP, and PVC on the sun-exposed side changed significantly over time (**Fig. 6**). After 12 months, the line density increased from 2.85 to 9.23 mm/mm² for PE and 4.16 to 8.47 mm/mm² for PP ($p < 0.05$, **Fig. 6A, D**). Similarly, the texture index on the sun-exposed side of PP increased from 0.096 to 0.31 ($p < 0.05$, **Fig. 6E**), whereas there was no significant change on the shaded side. PVC showed visible bubbles and fluctuations in the texture index after 8 month, but there was no noticeable change on the shaded side (**Fig. 6H**). Infrared spectroscopy showed pronounced changes in carbonyl groups on the surfaces of the plastic fragments (**Fig. S5**). The carbonyl index (CI) increased significantly across all materials, i.e., from 0.50 to 1.70 (PE), 0.18 to 1.10 (PP), and 0.45 to 1.57 (PVC) ($p < 0.05$, **Fig. 6C, F, I**). This result confirmed the occurrence of oxidative degradation on the sun-exposed sides. The formation of carbonyl groups and changes in the CI indicated photo-oxidation. Differences in crack patterns between PP and PE were attributed to variations in polymer structure and crystallinity [55]. For PVC, UV exposure led to discoloration and oxidation, producing a bubbly due to the release of gases such as chlorine [56].

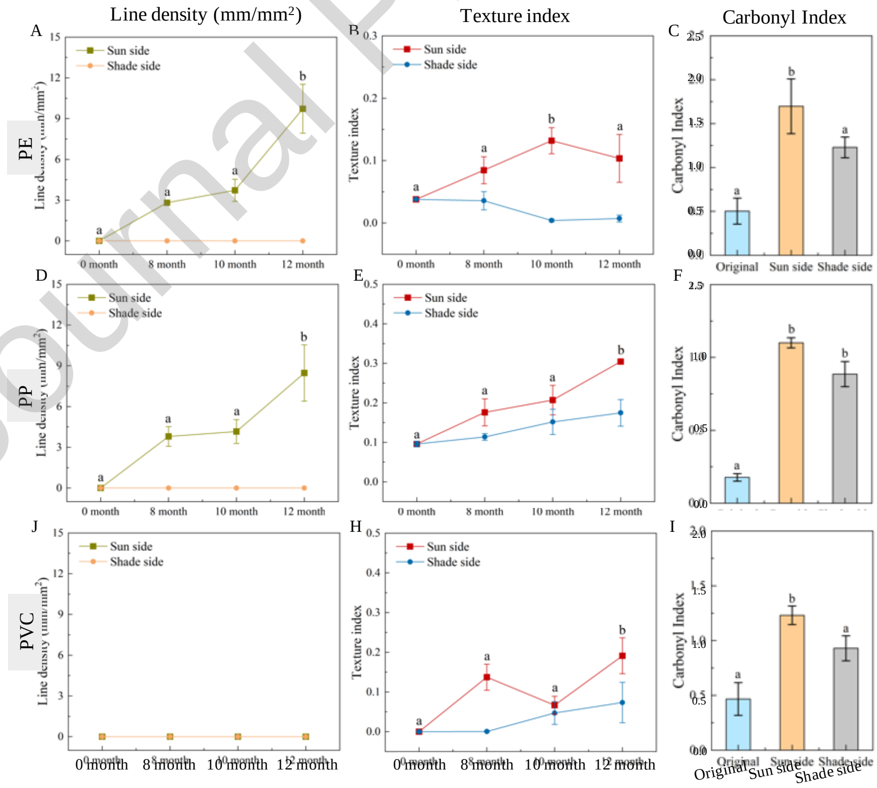

Fig. 6. Quantitative analysis of surface texture and aging characteristics on the sun side and shaded sides of polyethylene (PE), polypropylene (PP), and polyvinyl chloride (PVC) sheets after outdoor weathering. (Different lowercase letters indicate significant differences, $p < 0.05$)

3.4 The significance of exploring two-sided differences in plastic fragments

The two-sided weathering differences of beach plastic debris are common but often overlooked in environmental studies. Much of the existing research on plastic aging and fragmentation focused on one of the sides and neglects the potential impacts of the other side. This one-sided approach may lead to an incomplete understanding of how plastic fragments interact with the environment. A comprehensive study of both sides is necessary to fully reveal the mechanisms of action of natural aging and fragmentation.

Exploring two-sided weathering differences in beach plastic fragments enhanced our understanding of aging and fragmentation mechanisms. Firstly, the surface morphology of plastic fragments reflects key factors regarding their environmental life cycle and exposure condition. The formation of cracks and other weathering characteristics in plastic debris is caused by sunlight and ultraviolet (UV) radiation. Secondly, the plastic fragments are usually affected by uneven factors, leading to two-sided weathering differences. The side with rich texture characteristics was more likely to face sunlight, while the side with biological attachment was more often exposed to seawater. Thirdly, this study also provided critical insights for developing more accurate models to predict plastic degradation as proposed for the United Nations Sustainable Development Goals (SDGs) (**Text S2**) [57].

It is important to note that the real environmental conditions can't be fully confirmed, so most simulated studies have certain limitations. We suggest that multiple natural settings should be considered in future research to deepen understanding of the degradation of plastic debris in different environments.

4 Conclusions

In this study, we systematically investigated the two-sided weathering differences of plastic fragments through field investigations and outdoor experiments. The results showed significant weathering differences between the two sides of plastic fragments through field investigation and quantitative analysis. Moreover, the outdoor aging experiments showed that sunlight and UV radiation primarily led to photo-oxidative degradation. From these results, we can infer that the side with cracks or discoloration was more likely to face sunlight, while the side with biological attachment was more often exposed to seawater. This study provided critical insights for creating more accurate models to predict plastic degradation, aiding global strategies for mitigating plastic pollution.

CRediT authorship contribution statement

Bo Hu: Conceptualization, Data curation, Investigation, Methodology, Visualization, Validation, Writing – original draft. Mui-Choo Jong: Investigation, Methodology, Writing – review & editing. João Frias: Investigation, Methodology, Writing – review & editing. Irina Chubarenko: Investigation, Methodology, Writing – review & editing. Gabriel Enrique De-la-Torre: Investigation, Methodology. Prabhu Kolandhasamy: Investigation, Methodology. Md. Jaker Hossain: Investigation, Methodology. Elena Esiukova: Investigation, Methodology. Lei Su: Investigation, Methodology, Data curation, Writing – review & editing. Hua Deng: Investigation, Methodology, Data curation, Writing – review & editing. Wenjun Zhao: Investigation,

Methodology. Yifan Zheng: Investigation, Methodology. Huahong Shi: Resources, Supervision, Writing – review & editing.

Acknowledgment

This research was supported by grants from the National Key R&D Program of China (2023YFE0121500), National Natural Science Foundation of China (42207444), and Open Research Fund of the State Key Laboratory of Estuarine and Coastal Research (SKLEC-KF202311). Dr Frias acknowledges the JPI Oceans MicroplastiX project (PBA/PL/20/02) for their financial support to developing this work in collaboration with international partners. Thanks to Dr. Ma Cuizhu for Writing – review & editing.

Declaration of Competing Interest

The authors declare that they have no known competing financial interests or personal relationships that could have appeared to influence the work reported in this paper.

References

[1]. Jambeck JR, Geyer R, Wilcox C, Siegler TR, Perryman M, Andrady A, et al. Plastic waste inputs from land into the ocean. Science 2015;347(6223):768-771. DOI: 10.1126/science.1260352.

[2]. Napper IE, Thompson RC. Plastic Debris in the Marine Environment: History and Future Challenges. Global Challenges 2020;4(6):1900081. DOI: 10.1002/gch2.201900081.

[3]. Lomonaco T, Manco E, Corti A, La Nasa J, Ghimenti S, Biagini D, et al. Release of harmful volatile organic compounds (VOCs) from photo-degraded plastic debris: A neglected source of environmental pollution. Journal of Hazardous Materials 2020;394:122596. DOI: 10.1016/j.jhazmat.2020.122596.

[4]. Shi H, Frias J, Sayed AE-DH, De-la-Torre GE, Jong M-C, Uddin SA, et al. Small plastic fragments: A bridge between large plastic debris and micro- & nano-plastics. Trac-Trends in Analytical Chemistry 2023;168:117308. DOI: 10.1016/j.trac.2023.117308.

[5]. Landrigan PJ, Stegeman JJ, Fleming LE, Allemand D, Anderson DM, Backer LC, et al. Human health and ocean pollution. Annals of Global Health 2020;86(1):1-64. DOI: 10.5334/aogh.2831.

[6]. Nor NHM, Kooi M, Diepens NJ, Koelmans AA. Lifetime accumulation of microplastic in children and adults. Environmental Science & Technology 2021;55(8):5084-5096. DOI: 10.1021/acs.est.0c07384.

[7]. Wang L, Wu W-M, Bolan NS, Tsang DCW, Li Y, Qin M, et al. Environmental fate, toxicity and risk management strategies of nanoplastics in the environment: Current status and future perspectives. Journal of Hazardous Materials 2021;401:123415. DOI: 10.1016/j.jhazmat.2020.123415.

[8]. Wardlaw CM, Corcoran PL, Neff BD. Factors influencing the variation of microplastic uptake in demersal fishes from the upper Thames River Ontario. Environmental Pollution 2022;313:120095. DOI: 10.1016/j.envpol.2022.120095.

[9]. Lu QW, Zhou Y, Sui Q, Zhou YB. Mechanism and characterization of microplastic aging process: A review. Frontiers of Environmental Science & Engineering 2023;17(8):100-118. DOI: 10.1007/s11783-023-1700-6.

[10]. Scott JW, Turner A, Prada AF, Zhao L. Heterogeneous weathering of polypropylene in the marine environment. Science of the Total Environment 2022;812:152308. DOI: 10.1016/j.scitotenv.2021.152308.

[11]. Binda G, Zanetti G, Bellasi A, Spanu D, Boldrocchi G, Bettinetti R, et al. Physicochemical and biological ageing processes of (micro)plastics in the environment: a multi-tiered study on polyethylene. Environmental Science and Pollution Research 2022;30(3):6298-6312. DOI: 10.1007/s11356-022-22599-4.

[12]. Rizzo M, Corbau C, Lane B, Malkin SY, Bezzi V, Vaccaro C, et al. Examining the dependence of macroplastic fragmentation on coastal processes (Chesapeake Bay, Maryland). Marine Pollution Bulletin 2021;169:112510. DOI: 10.1016/j.marpolbul.2021.112510.

[13]. Ding X, Chen Y, Chao CA, Wu Y-L, Wang Y. Control the Mechanical Properties and Degradation of Poly(Glycerol Sebacate) by Substitution of the Hydroxyl Groups with Palmitates. Macromolecular Bioscience 2020;20(9):202000101. DOI: 10.1002/mabi.202000101.

[14]. Deng H, Su L, Zheng Y, Du F, Liu Q, Zheng J, et al. Crack patterns of environmental plastic fragments. Environmental Science & Technology 2022;56(10):6399-6414. DOI: 10.1021/acs.est.1c08100.

[15]. Salomez M, George M, Fabre P, Touchaleaume F, Cesar G, Lajarrige A, et al. A comparative study of degradation mechanisms of PHBV and PBSA under laboratory-scale composting conditions. Polymer Degradation and Stability 2019;167:102-113. DOI: 10.1016/j.polymdegradstab.2019.06.025.

[16]. Teymouri Y, Adams A, Bluemich B. Compact low-field NMR: Unmasking morphological changes from solvent-induced crystallization in polyethylene. European Polymer Journal 2016;80:48-57. DOI: 10.1016/j.eurpolymj.2016.04.037.

[17]. Zheng Y, Zhu J, Li J, Li G, Shi H. Burrowing invertebrates induce fragmentation of mariculture Styrofoam floats and formation of microplastics. Journal of Hazardous Materials 2023;447:130764. DOI: 10.1016/j.jhazmat.2023.130764.

[18]. Commission O. Guideline for monitoring marine litter on the beaches in the OSPAR maritime area (Edition 1.0). OSPAR Commission, 2010. (ISBN 90 3631 973 9.).

[19]. Xu JL, Thomas KV, Luo ZS, Gowen AA. FTIR and Raman imaging for microplastics analysis: State of the art, challenges and prospects. Trac-Trends in Analytical Chemistry 2019;119:115629. DOI: 10.1016/j.trac.2019.115629.

[20]. Primpke S, Cross RK, Mintenig SM, Simon M, Vianello A, Gerdts G, et al. Toward the Systematic Identification of Microplastics in the Environment: Evaluation of a New Independent Software Tool (siMPle) for Spectroscopic Analysis. Applied Spectroscopy 2020;74(9):1127-1138. DOI: 10.1177/0003702820917760.

[21]. Michel APM, Morrison A, Colson BC, Marx CT, White HK. Comparison of Laboratory Analytical Techniques for the Rapid Identification of Marine Plastics. OCEANS 2019 - Marseille 2019:8867289. DOI: 10.1109/oceanse.2019.8867289.

[22]. Nielsen MS, Nikolov I, Kruse EK, Garnaes J, Madsen CB. Quantifying the influence of surface texture

and shape on structure from motion 3D reconstructions. Sensors 2023;23(1):23010178. DOI: 10.3390/s23010178.

[23]. Josso B, Burton DR, Lalor MJ. Texture orientation and anisotropy calculation by Fourier transform and principal component analysis. Mechanical Systems and Signal Processing 2005;19(5):1152-1161. DOI: 10.1016/j.ymssp.2004.07.005.

[24]. Bouwman H, Evans SW, Cole N, Yive N, Kylin H. The flip-or-flop boutique: Marine debris on the shores of St Brandon's rock, an isolated tropical atoll in the Indian Ocean. Marine Environmental Research 2016;114:58-64. DOI: 10.1016/j.marenvres.2015.12.013.

[25]. Bhat MA, Gedik K, Gaga EO. Atmospheric micro (nano) plastics: future growing concerns for human health. Air Quality Atmosphere and Health 2023;16(2):233-262. DOI: 10.1007/s11869-022-01272-2.

[26]. Resmerita A-M, Coroaba A, Darie R, Doroftei F, Spiridon I, Simionescu BC, et al. Erosion as a possible mechanism for the decrease of size of plastic pieces floating in oceans. Marine Pollution Bulletin 2018;127:387-395. DOI: 10.1016/j.marpolbul.2017.12.025.

[27]. Casabianca S, Capellacci S, Penna A, Cangiotti M, Fattori A, Corsi I, et al. Physical interactions between marine phytoplankton and PET plastics in seawater. Chemosphere 2020;238:124560. DOI: 10.1016/j.chemosphere.2019.124560.

[28]. Lacerda AL, Frias J, Pedrotti ML. Tardigrades in the marine plastisphere: New hitchhikers surfing plastics. Marine Pollution Bulletin 2024;200:116071. DOI: 10.1016/j.marpolbul.2024.116071.

[29]. El-Sherif DM, Eloffy MG, Elmesery A, Abouzid M, Gad M, El-Seedi HR, et al. Environmental risk, toxicity, and biodegradation of polyethylene: a review. Environmental Science and Pollution Research 2022;29(54):81166-81182. DOI: 10.1007/s11356-022-23382-1.

[30]. Lv S, Li Y, Zhao S, Shao Z. Biodegradation of Typical Plastics: From Microbial Diversity to Metabolic Mechanisms. International Journal of Molecular Sciences 2024;25(1). DOI: 10.3390/ijms25010593.

[31]. Falkenstein P, Graesing D, Bielytskyi P, Zimmermann W, Matysik J, Wei R, et al. UV pretreatment impairs the enzymatic degradation of polyethylene terephthalate. Frontiers in Microbiology 2020;11:00689. DOI: 10.3389/fmicb.2020.00689.

[32]. Vega-Herrera A, Llorca M, Savva K, León VM, Abad E, Farré M. Screening and Quantification of

Micro(Nano)Plastics and Plastic Additives in the Seawater of Mar Menor Lagoon. Frontiers in Marine Science 2021;8:697424. DOI: 10.3389/fmars.2021.697424.

[33]. Cheng JG, Jacquin J, Conan P, Pujo-Pay M, Barbe V, George M, et al. Relative Influence of Plastic Debris Size and Shape, Chemical Composition and Phytoplankton-Bacteria Interactions in Driving Seawater Plastisphere Abundance, Diversity and Activity. Frontiers in Microbiology 2021;11. DOI: 10.3389/fmicb.2020.610231.

[34]. Feng Z, Song G-L, Wang ZM, Xu Y, Zheng D, Wu P, et al. Salt crystallization-assisted degradation of epoxy resin surface in simulated marine environments. Progress in Organic Coatings 2020;149. DOI: 10.1016/j.porgcoat.2020.105932.

[35]. McBride SA, Dash S, Varanasi KK. Evaporative Crystallization in Drops on Superhydrophobic and Liquid-Impregnated Surfaces. Langmuir 2018;34(41):12350-12358. DOI: 10.1021/acs.langmuir.8b00049.

[36]. Reineccius J, Schoenke M, Waniek JJ. Abiotic Long-Term Simulation of Microplastic Weathering Pathways under Different Aqueous Conditions. Environmental Science & Technology 2022;57:963-975. DOI: 10.1021/acs.est.2c05746.

[37]. Meides N, Menzel T, Poetzschner B, Loeder MGJ, Mansfeld U, Strohriegl P, et al. Reconstructing the environmental degradation of polystyrene by accelerated weathering. Environmental Science & Technology 2021;55(12):7930-7938. DOI: 10.1021/acs.est.0c07718.

[38]. Gewert B, Plassmann MM, MacLeod M. Pathways for degradation of plastic polymers floating in the marine environment. Environmental Science-Processes & Impacts 2015;17(9):1513-1521. DOI: 10.1039/c5em00207a.

[39]. Gewert B, Plassmann M, Sandblom O, MacLeod M. Identification of chain scission products released to water by plastic exposed to ultraviolet light. Environmental Science & Technology Letters 2018;5(5):272-276. DOI: 10.1021/acs.estlett.8b00119.

[40]. Cooper DA, Corcoran PL. Effects of mechanical and chemical processes on the degradation of plastic beach debris on the island of Kauai, Hawaii. Marine Pollution Bulletin 2010;60(5):650-654. DOI: 10.1016/j.marpolbul.2009.12.026.

[41]. Rillig MC, Kim SW, Kim T-Y, Waldman WR. The Global Plastic Toxicity Debt. Environmental Science & Technology 2021;55(5):2717-2719. DOI: 10.1021/acs.est.0c07781.

[42]. Weinstein JE, Crocker BK, Gray AD. From macroplastic to microplastic: Degradation of high-density polyethylene, polypropylene, and polystyrene in a salt marsh habitat. Environmental Toxicology and Chemistry 2016;35(7):1632-1640. DOI: 10.1002/etc.3432.

[43]. Corcoran PL, Belontz SL, Ryan K, Walzak MJ. Factors Controlling the Distribution of Microplastic Particles in Benthic Sediment of the Thames River, Canada. Environmental Science & Technology 2020;54(2):818-825. DOI: 10.1021/acs.est.9b04896.

[44]. Pincus LN, Pattammattel A, Leshchev D, Zhao K, Stavitski E, Chu YS, et al. Rapid Accumulation of Soil Inorganics on Plastics: Implications for Plastic Degradation and Contaminant Fate. Environmental Science & Technology Letters 2023;10(6):538-542. DOI: 10.1021/acs.estlett.3c00241.

[45]. Sun J, Zheng H, Xiang H, Fan J, Jiang H. The surface degradation and release of microplastics from plastic films studied by UV radiation and mechanical abrasion. Science of the Total Environment 2022;838:156369. DOI: 10.1016/j.scitotenv.2022.156369.

[46]. Rani R, Khurana M, Kumar A, Kumar N. Big data dimensionality reduction techniques in IoT: review, applications and open research challenges. Cluster Computing-the Journal of Networks Software Tools and Applications 2022;25(6):4027-4049. DOI: 10.1007/s10586-022-03634-y.

[47]. Zhang X, Pi H, Guo S. The Effect of High Intensity UV Irradiation on Color Behavior of Poly(Vinyl Chloride). Journal of Macromolecular Science Part B-Physics 2012;51(7):1303-1321. DOI: 10.1080/00222348.2011.627828.

[48]. Bajer K, Braun U. Different aspects of the accelerated oxidation of polypropylene at increased pressure in an autoclave with regard to temperature, pretreatment and exposure media. Polymer Testing 2014;37:102-111. DOI: 10.1016/j.polymertesting.2014.05.006.

[49]. Wang L, Zhang J, Huang W, He Y. Laboratory simulated aging methods, mechanisms and characteristic changes of microplastics: A review. Chemosphere 2023;315:137744. DOI: 10.1016/j.chemosphere.2023.137744.

[50]. Ainali NM, Bikiaris DN, Lambropoulou DA. Aging effects on low- and high-density polyethylene,

polypropylene and polystyrene under UV irradiation: An insight into decomposition mechanism by Py-GC/MS for microplastic analysis. Journal of Analytical and Applied Pyrolysis 2021;158. DOI: 10.1016/j.jaap.2021.105207.

[51]. An YJ, Kajiwara T, Padermshoke A, Nguyen TV, Feng SN, Masunaga H, et al. Photooxidative degradation and fragmentation behaviors of oriented isotactic polypropylene. Polymer Journal 2024;56(4):379-389. DOI: 10.1038/s41428-023-00876-4.

[52]. Wang C, Xian Z, Jin X, Liang S, Chen Z, Pan B, et al. Photo-aging of polyvinyl chloride microplastic in the presence of natural organic acids. Water Research 2020;183. DOI: 10.1016/j.watres.2020.116082.

[53]. Li Y, Zeng Q, Sun Y, Liu Q, Yang Q, Hao Y, et al. Revealing the complex oxidation behavior of extracellular polymeric substances interacted with pristine and aged polypropylene microplastics. Journal of Water Process Engineering 2024;63. DOI: 10.1016/j.jwpe.2024.105492.

[54]. Ouyang Z, Zhang Z, Jing Y, Bai L, Zhao M, Hao X, et al. The photo-aging of polyvinyl chloride microplastics under different UV irradiations. Gondwana Research 2022;108:72-80. DOI: 10.1016/j.gr.2021.07.010.

[55]. Real LEP, Ferraria AM, do Rego AMB. Comparison of different photo-oxidation conditions of poly(vinyl chloride) for outdoor applications. Polymer Testing 2008;27(6):743-751. DOI: 10.1016/j.polymertesting.2008.05.009.

[56]. Hankett JM, Collin WR, Chen Z. Molecular structural changes of plasticized PVC after UV light exposure. Journal of Physical Chemistry B 2013;117(50):16336-16344. DOI: 10.1021/jp409254y.

[57]. Walker TR. (Micro)plastics and the UN Sustainable Development Goals. Current Opinion in Green and Sustainable Chemistry 2021;30:100497. DOI: 10.1016/j.cogsc.2021.100497.

Graphical Abstract

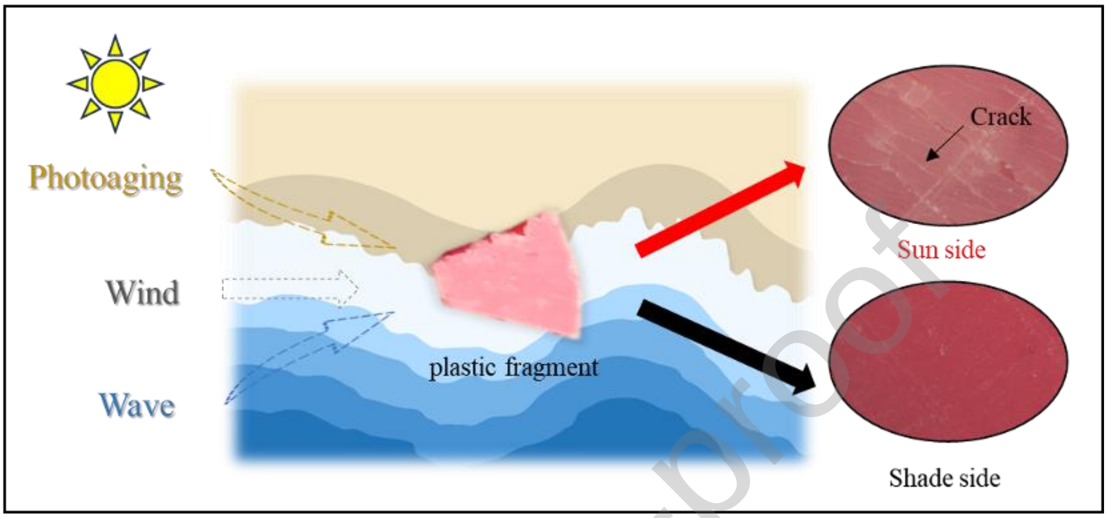

Declaration of interests

√ The authors declare that they have no known competing financial interests or personal relationships that could have appeared to influence the work reported in this paper.

Highlights:

- Plastic fragments exhibited divergent weathering changes on their two sides.
- Quantification analysis further validated such weathering differences.
- Ultraviolet radiation was supposed to accelerate aging and increase weathering differences.
- Consideration of both sides is critical for understanding plastic weathering.